Size of Plastic Events in Strained Amorphous Solids at Finite Temperatures

H. G. E. Hentschel,* Smarajit Karmakar, Edan Lerner, and Itamar Procaccia
Department of Chemical Physics, The Weizmann Institute of Science, Rehovot 76100, Israel
(Received 11 August 2009; published 11 January 2010)

We address the system-size dependence of plastic flow events when an amorphous solid is put under a fixed external strain rate at a finite temperature. For small system sizes at low strain rates and low temperatures the magnitude of plastic events grows with the system size. We explain, however, that this must be a finite-size effect; for larger systems there exist two crossover length scales ξ_1 and ξ_2, the first determined by the elastic time scale and the second by the thermal energy scale. For systems of size $L \gg \xi$ there must exist $(L/\xi)^d$ uncorrelated plastic events which occur simultaneously. We present a scaling theory that culminates with the dependence of the crossover scales on temperature and strain rate. Finally, we relate these findings to the temperature and size dependence of the stress fluctuations. We comment on the importance of these considerations for theories of elastoplasticity.

DOI: 10.1103/PhysRevLett.104.025501 PACS numbers: 61.43.Fs, 81.05.Kf

Introduction.—The issues of the statistical correlations of plastic flow events in strained amorphous solids are central to the possible form of the dynamical theory of elastoplasticity [1–6]. As such, they have been at the center of extensive research in recent years [7–11]. The crucial question is whether these events are spatially localized and statistically independent, as assumed often in the theoretical development, or whether they are statistically correlated to form extended events that depend on the system size. Of particular relevance to the present Letter is Ref. [12], in which the authors studied the question for zero temperature as a function of the strain rate. At low strain rates $\dot{\gamma}$ the plastic events were shown to be spatially correlated with a system-size dependence. At high strain rates (compared to elastic relaxation times) the correlations were cut off proportional to $\dot{\gamma}^{-1/d}$, where d is the space dimension. Two crucial questions that remain are (i) what is the effect of temperature on this issue? (should temperature fluctuations also cut off the statistical correlations?) and (ii) if temperature effects do cut off the magnitude of plastic flow events, which of the cutoffs dominates at a given temperature and strain rate?

The aim of this Letter is to address these two questions. We will show that temperature effects are as important, if not more important, in checking the magnitude of plastic events as the effect of a finite $\dot{\gamma}$. We will present below some quantitative estimates of the various effects to compare their efficacy in bounding the magnitude of plastic flow events at a given temperature and strain rate.

Summary of the athermal quasistatic simulations.—At athermal conditions $T = 0$ an amorphous solid consisting of N particles of mass m and mass density ρ in a volume $V = L^d$ is subjected to very slow strain rate $\dot{\gamma}$ (quasistatic in the limit) tending to set up an elastoplastic steady state in which short elastic intervals in which the energy and the stress slowly increase are interrupted by plastic flow events during which the energy and the stress decrease on the short time scale of elastic relaxation. During the steady state, one can measure accurately the average shear stress drops $\langle \Delta\sigma \rangle$ or the average energy drops $\langle \Delta U \rangle$. In both two dimensions [11] and three dimensions [13] it was found that these averages depend on N as power laws,

$$\langle \Delta U \rangle = \bar{\epsilon} N^{\alpha}, \qquad \langle \Delta\sigma \rangle = s N^{\beta}, \tag{1}$$

with $\alpha > 0$ and $\beta < 0$, where $\bar{\epsilon}$ is the mean energy drop per particle and s is a stress scale to be computed below. A scaling relation $\alpha - \beta = 1$ follows from the average energy balance equation, cf. Ref. [11],

$$\sigma_Y \langle \Delta\sigma \rangle V/\mu = \langle \Delta U \rangle, \tag{2}$$

where σ_Y is the flow stress (the mean stress in the athermal steady state) and μ is the shear modulus. The actual values of the exponents α and β can depend on the details of the interparticle potential. Typical values of α are a bit less than 0.4 in two dimensions [11] and a bit more than 0.4 in three dimensions [13]. In Ref. [11], it was shown that the number of particles participating in a plastic flow event scales like $\langle \Delta U \rangle$.

The effect of finite strain rate.—As noted in the introduction, Ref. [12] showed that finite strain rates may cut off the magnitude of plastic flow events. To understand this effect, we start by substituting Eq. (1) in Eq. (2) to obtain the scale s. With $\langle \lambda \rangle$ being the mean interparticle distance, we write:

$$s = \frac{\bar{\epsilon}\mu}{\sigma_Y \langle \lambda \rangle^d} = \frac{\bar{\epsilon}\mu\rho}{\sigma_Y m}. \tag{3}$$

Consider next the rate at which work is being done at the system and balance it by the energy dissipation in the steady state,

$$\sigma_Y \dot{\gamma} V = \langle \Delta U \rangle / \tau_{\rm pl}, \tag{4}$$

where $\tau_{\rm pl}$ is the average time between plastic flow events. This time is estimated as the elastic rise time which is

$$\tau_{\rm pl} \sim \frac{\langle \Delta\sigma \rangle}{\mu \dot{\gamma}} \sim \frac{\bar{\epsilon} N^{\beta}}{\sigma_Y \langle \lambda \rangle^d \dot{\gamma}}. \quad (5)$$

We increase our confidence in this estimate by substituting it into Eq. (4) together with the other estimates to find perfect consistency.

Next we note that $\tau_{\rm pl}$ decreases when N increases. On the other hand, there exists another crucial time scale in the system, which is the elastic relaxation time $\tau_{\rm el} \sim L/c$, where c is the speed of sound $c = \sqrt{\mu/\rho}$. Obviously, this time scale *increases* with N like $N^{1/d}$. Therefore, there will be a typical scale ξ_1 such that for a system of scale $L = \xi_1$ these times cross. At that size, the system cannot equilibrate its elastic energy before another event is triggered, and multiple avalanches must be occurring simultaneously in different parts of the system, each of which has a bounded magnitude. We estimate ξ_1 from $\tau_{\rm el} \sim \tau_{\rm pl}$, finding

$$(\xi_1/c) \sim \frac{\epsilon [N(\xi_1)]^{\beta}}{\sigma_Y \langle \lambda \rangle^d \dot{\gamma}} \sim \frac{\epsilon [\xi/\langle \lambda \rangle]^{d\beta}}{\sigma_Y \langle \lambda \rangle^d \dot{\gamma}}. \quad (6)$$

Using now the obvious fact that $N(\xi_1) \sim (\xi_1/\langle \lambda \rangle)^d$, we compute

$$\frac{\xi_1}{\langle \lambda \rangle} \sim \left[\left(\frac{\bar{\epsilon}}{\sigma_Y \langle \lambda \rangle^d} \right) \left(\frac{c}{\langle \lambda \rangle \dot{\gamma}} \right) \right]^{1/(1-\beta d)}. \quad (7)$$

We observe the singularity for quasistatic strain when $\dot{\gamma} \to 0$, where ξ_1 tends to infinity, in agreement with the results of quasistatic calculations. At low temperatures, before the thermal energy scale becomes important, the size of plastic flow events can be huge indeed. Note that there exists a difference between our estimate of ξ_1 and that of Ref. [12]; this stems from our attempt to put a more stringent constraint to see how big the system can be while separating individual plastic drops. We show next that thermal effects put a much more stringent bound on the magnitude of plastic flow events.

The effect of finite temperatures.—During a plastic drop, the energy released quickly spreads out in the system on the time scale of elastic waves. Thus every particle shares an energy of the order of $\bar{\epsilon} N^{\alpha}/N = \bar{\epsilon} N^{\beta}$. On the other hand, the typical scale of thermal energy per particle is $k_B T$, where k_B is Boltzmann's constant. We thus expect thermal effects to start overwhelming the statistics of athermal plastic events when

$$\bar{\epsilon} N^{\beta} \sim k_B T. \quad (8)$$

This equality will hold when the system size $L = \xi_2$, where $(\xi_2/\langle \lambda \rangle)^d = N$. Substituting the last equality in Eq. (8) and then solving for ξ_2, we find

$$\xi_2/\langle \lambda \rangle = [k_B T/\bar{\epsilon}]^{1/d\beta}. \quad (9)$$

Recalling that $\beta = \alpha - 1$ is negative, we again notice the singularity at $T \to 0$ in agreement with the athermal quasistatic simulations.

A model glass example.—To put some size estimates on these crucial length scales and to test their consequences, we need to choose a model glass. To this aim, we employ a model system with point particles of equal mass m and positions $\boldsymbol{r}_i$ in three dimensions interacting via a pairwise interaction potential. In our three-dimensional simulations, each particle i is assigned an interaction parameter λ_i from a normal distribution with mean $\langle \lambda \rangle$. The variance is governed by the polydispersity parameter $\Delta = 15\%$, where $\Delta^2 = \frac{\langle (\lambda_i - \langle \lambda \rangle)^2 \rangle}{\langle \lambda \rangle^2}$. With the definitions $r_{ij} = |\boldsymbol{r}_i - \boldsymbol{r}_j|$ and $\lambda_{ij} = \frac{1}{2}(\lambda_i + \lambda_j)$, the potential assumes the form

$$U(r_{ij}) = \begin{cases} \epsilon \left[\left(\frac{\lambda_{ij}}{r_{ij}} \right)^k - \frac{k(k+2)}{8} \left(\frac{B_0}{k} \right)^{(k+4)/(k+2)} \left(\frac{r_{ij}}{\lambda_{ij}} \right)^4 + \frac{B_0(k+4)}{4} \left(\frac{r_{ij}}{\lambda_{ij}} \right)^2 - \frac{(k+2)(k+4)}{8} \left(\frac{B_0}{n} \right)^{k/(k+2)} \right], & r_{ij} \le \lambda_{ij} \left(\frac{k}{B_0} \right)^{1/(k+2)} \\ 0 & r_{ij} > \lambda_{ij} \left(\frac{k}{B_0} \right)^{1/(k+2)} \end{cases}. \quad (10)$$

In our two-dimensional simulations below, we use the same potential but choose a binary mixture model with "large" and "small" particles such that $\lambda_{LL} = 1.4$, $\lambda_{LS} = 1.18$, and $\lambda_{SS} = 1.00$. Below the units of length, energy, mass, and temperature are $\langle \lambda \rangle$, ϵ, m, and ϵ/k_B, where k_B is Boltzmann's constant. The time units τ_0 are accordingly $\tau_0 = \sqrt{(m\langle \lambda \rangle^2/\epsilon)}$. The motivation of this lengthy form of the potential is to have continuous first and second derivatives at the cutoff of $r_{ij} = \lambda_{ij}(k/B_0)^{1/(k+2)}$. In the present simulations, we chose $k = 10$, $B_0 = 0.2$. In the 3D simulations below, the mass density $\rho \equiv mN/V = 1.3$, whereas in 2D, $\rho = 0.85$. In all cases the boundary conditions are periodic and thermostatting is achieved with the Berendsen scheme [14]. In Fig. 1, we present a typical 3D equilibrium configuration of the system with $N = 65\,356$. We measured for this 3D system the shear modulus $\mu = 15.7$, and therefore the speed of sound is $c \approx 3.5$. The value of σ_Y at $T = 0$ is about 0.7, and the typical value of σ_∞ at higher temperatures is of the order of 0.5.

The estimate of ξ_1 depends, of course, on $\dot{\gamma}$. In our 3D simulations, we have used $\dot{\gamma} = 5 \times 10^{-5}$, and for the given values of the speed of sound and of σ_Y, we estimate $\xi_1/\langle \lambda \rangle \sim 2 \times 10^5$, which translates to about 10^{16} particles. Obviously, this system size is hugely beyond the capabilities of molecular simulations. One could in principle increase $\dot{\gamma}$, but not beyond $\sigma_y/(\sqrt{\rho\mu}L)$ [15]. It therefore remains elusive to demonstrate the crossover due to the elastic time scale in numerical simulations. Nevertheless, one should remember that in developing an athermal theory of elastoplasticity, the plastic flow events are very large, a fact that cannot be disregarded with impunity.

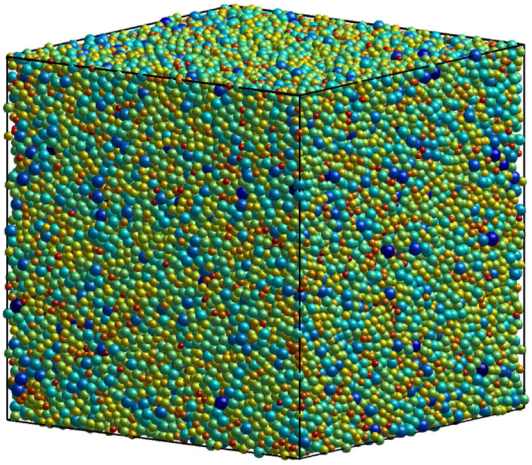

FIG. 1 (color online). A typical equilibrium configuration with 65 356 particles. The particles are all point objects, and the ball around each particle is of radius λ_i.

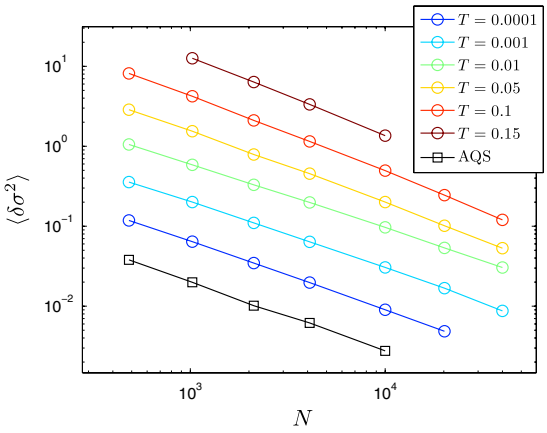

FIG. 2 (color online). The variance of the stress fluctuations as a function of the system size N for a 2D system and for various temperatures. The first power law (data in squares) is obtained under athermal quasistatic conditions where we determine for the present model $\beta = -0.61$, $\theta = -0.40$. The other plots go up in temperature as indicated. The plots are displaced by a fixed amount for clarity. Note that the slope becomes more negative as the temperature increases.

The crossover scale due to thermal energies is very well within the range of system size available in numerical simulations. Making the plausible estimate $\bar{\epsilon} \approx \epsilon$, we see that already at $T = 10^{-3}$ $\xi_2/\langle\lambda\rangle$ is estimated (for $\beta = -8/15$ in three dimensions [13]) as $\xi_2 \approx 10^2$, which translates to just 1×10^6 particles. For $T = 10^{-2}$, this estimate drops down to about 1000 particles. Thus, we expect a very rapid crossover from correlated avalanches to uncorrelated ones as the temperature rises above 10^{-3}.

Demonstration of the thermal crossover.—A very interesting and direct way of demonstrating the crossover due to thermal effects is provided by measurements of the variance of the stress fluctuations as a function of the temperature and the system size. This variance is defined by $\langle \delta\sigma^2 \rangle \equiv \langle (\sigma - \sigma_\infty)^2 \rangle$, where σ_∞ is the mean stress in the thermal steady state. In Figs. 2 and 3, we display 2D and 3D measurements of this quantity which is obtained by averaging the square of the microscopic stress fluctuations in long stretches of elastoplastic steady states of the models described above at a fixed $\dot{\gamma} = 2.5 \times 10^{-5}$ in 2D and $\dot{\gamma} = 5 \times 10^{-5}$ in 3D. It is evident that the variance of the stress fluctuations decreases as a function of N. Under quasistatic and athermal conditions, the dependence is a power law

$$\langle \delta\sigma^2 \rangle \sim N^{2\theta}, \tag{11}$$

where $\theta \approx -0.4$ both in 2D and 3D. One should notice the difference between the exponent characterizing the N dependence of $\sqrt{\langle \delta\sigma^2 \rangle}$ and of the athermal mean plastic stress drop $\langle \Delta\sigma \rangle$ in the sense that $\theta \neq \beta$. This difference is due to very strong correlations between elastic increases and plastic drops. At higher temperatures, the data in Figs. 2 and 3 indicate a clear crossover to independent stress fluctuations in which $\langle \delta\sigma^2 \rangle \sim N^{-1}$ for high temperatures.

To capture the temperature and size dependence of the variance and to demonstrate unequivocally the thermal crossover, we first need to separate the thermal from the mechanical contributions to $\langle \delta\sigma^2 \rangle$. We write

$$\langle \delta\sigma^2 \rangle = \langle \delta\sigma^2 \rangle_T + \langle \widetilde{\delta\sigma^2} \rangle, \tag{12}$$

where $\langle \delta\sigma^2 \rangle_T$ denotes the thermal contribution which can be read from Eq. (10) of Ref. [16], i.e.,

$$\langle \delta\sigma^2 \rangle_T \approx \mu T/V. \tag{13}$$

For the mechanical part, we introduce a scaling function which exhibits a crossover according to Eq. (8). In other

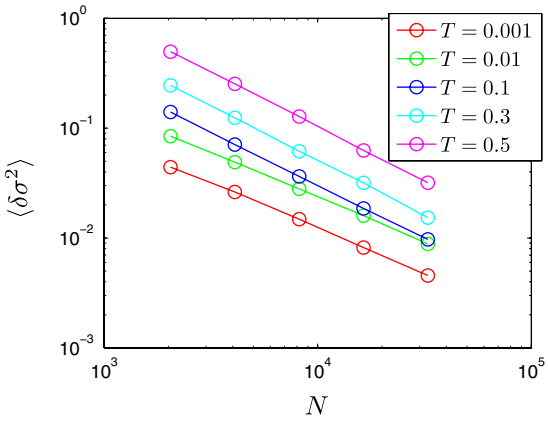

FIG. 3 (color online). The variance of the stress fluctuations as a function of the system size N for a 3D system and for various temperatures. The plots are displaced by a fixed amount for clarity. Note that the slope becomes more negative as the temperature increases.

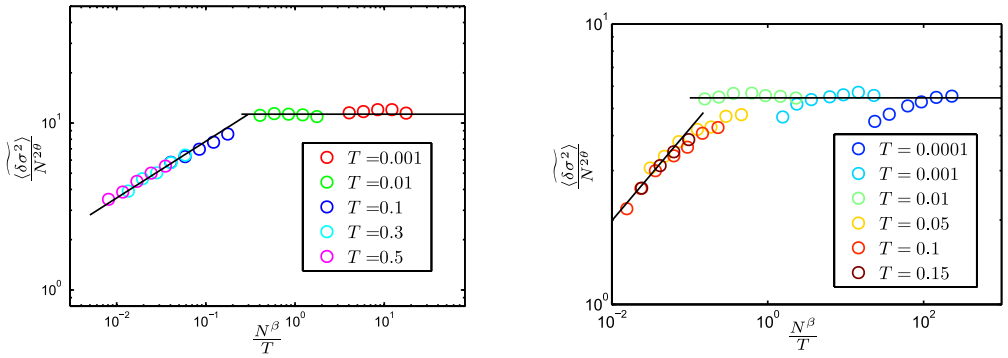

FIG. 4 (color online). The scaling function $g(x)$, cf. Eq. (15), for the 3D data (left panel) and the 2D data (right panel). Note the crossover for x of the order of unity as predicted by Eq. (8). The power-law decrease at low values of x is in agreement with the prediction of $\zeta \approx 0.33$ in both cases. The two black lines represent the theoretical prediction for the scaling function $g(x)$ for $x \ll 1$ and for $x \gg 1$. Note that the full scaling function depends on $\dot{\gamma}$, and the present one is an approximate version for $\dot{\gamma} \to 0$. This is the reason for the curved data sets of the low temperature runs.

words, we propose a scaling function $g(x)$ to describe the system size and temperature dependence of the mechanical part of the variance:

$$\langle\widetilde{\delta\sigma^2}\rangle(N,T) = s^2 N^{2\theta} g(\bar{\epsilon} N^\beta / k_B T). \tag{14}$$

The dimensionless scaling function $g(x)$ must satisfy

$$g(x) \to g_\infty \quad \text{for } x \to \infty \quad \text{and} \quad g(x) \to g_0 x^\zeta \quad \text{for } x \to 0. \tag{15}$$

The first of these requirements means that the fluctuations are in accordance with the athermal limit. The second means that after the crossover, the fluctuations of the stress become intensive, requiring $\zeta = -(1 + 2\theta)/\beta$. We compute $\zeta \approx 0.33$ in both 2D and 3D.

We present tests of the scaling function for both our 2D and 3D simulations in Fig. 4. Examining the scaling functions in Fig. 4, we see that although the data collapse is not perfect, the thermal crossover is demonstrated very well where expected, i.e., at values of x of the order of unity. The asymptotic behavior of the scaling functions agrees satisfactorily with the theoretical prediction for both the 2D and the 3D data.

We thus conclude this Letter by reiterating that the thermal crossover appears much more aggressive than the shear-rate crossover in cutting off the subextensive scaling of the shear fluctuations and mean drops. For macroscopic systems, it should be quite impossible to observe plastic events that are correlated over the system size except for extremely low temperatures in the nano-Kelvin range. On the other hand, nanoparticles of amorphous solids may show at low temperatures and low strain rates some rather spectacular correlated plastic events.

This work has been supported in part by the German Israeli Foundation, the Israel Science Foundation, and the Minerva Foundation, Munich, Germany.

*Present address: Department of Physics, Emory University, Atlanta, GA 30322, USA.

[1] A. S. Argon and H. Y. Kuo, Mater. Sci. Eng. **39**, 101 (1979).
[2] A. S. Argon, Acta Metall. **27**, 47 (1979).
[3] A. S. Argon and L. T. Shi, Philos. Mag. A **46**, 275 (1982).
[4] M. L. Falk and J. S. Langer, Phys. Rev. E **57**, 7192 (1998).
[5] P. Sollich, Phys. Rev. E **58**, 738 (1998).
[6] E. Bouchbinder, J. S. Langer, and I. Procaccia, Phys. Rev. E **75**, 036107 (2007); **75**, 036108 (2007).
[7] C. E. Maloney and A. Lemaitre, Phys. Rev. Lett. **93**, 016001 (2004).
[8] A. Tanguya, F. Leonforte, and J.-L. Barrat, Eur. Phys. J. E **20**, 355 (2006).
[9] C. E. Maloney and A. Lemaître, Phys. Rev. E **74**, 016118 (2006).
[10] C. E. Maloney and M. O. Robbins, Phys. Rev. Lett. **102**, 225502 (2009).
[11] E. Lerner and I. Procaccia, Phys. Rev. E **79**, 066109 (2009).
[12] A. Lemaitre and C. Caroli, Phys. Rev. Lett. **103**, 065501 (2009).
[13] N. P. Bailey, J. Schiøtz, A. Lemaître, and K. W. Jacobsen, Phys. Rev. Lett. **98**, 095501 (2007).
[14] M. P. Allen and D. J. Tildesley, *Computer Simulations of Liquids* (Oxford University Press, New York, 1991).
[15] Increasing $\dot{\gamma}$ beyond this value causes competition with the elastic relaxation time and a disruption of the linear shear profile.
[16] V. Ilyin, N. Makedonska, I. Procaccia, and N. Schupper, Phys. Rev. E **76**, 052401 (2007).